JOURNAL OF SOLID STATE CHEMISTRY 60, 297–304 (1985)

Chemical Bonding Interactions in Zr_2Al

R. J. KEMATICK* AND H. F. FRANZEN†

Ames Laboratory–DOE and Department of Chemistry, Iowa State University, Ames, Iowa 50011

AND D. K. MISEMER‡

Ames Laboratory–DOE and Department of Chemistry, Iowa State University, Ames, Iowa 50011

Received March 22, 1985; in revised form May 24, 1985

The electronic structure of Zr_2Al with the Ni_2In-type structure has been calculated by the method of W. Kohn and N. Rostoker (*Phys. Rev.* **91,** 1111 (1954)). The results include densities of states, both total and partial, and resolved according to the angular momentum quantum number, and calculated electron densities presented so as to display directional bonding characteristics of electrons in the valence and conduction regions of energy. It is concluded that: (1) the principal bonding involves aluminum *s*-type orbitals; (2) the aluminum *p*-type orbitals are principally nonbonding; and (3) the metallic interactions are principally between zirconium atoms.

Introduction

The understanding of electronic interactions in early transition-metal, solid, binary compounds has been greatly enhanced by recent calculations of the band structures of compounds with elementary structure types (*1–3*). Because the early transition-metal aluminides are of technological interest owing to their refractory and corrosion-resistant nature, it was decided to undertake a similar calculation for a zirconium aluminide. A second motivation for examining the electronic structure of a zirconium aluminide was the general observation that the stoichiometries and structures of zirconium aluminides are quite unlike those of other main-group compounds with zirconium, such as the sulfides. This observation suggests differing roles for the main group element orbitals in forming chemical bonds, a difference that is amenable to theoretical analysis. The results of this study show that, on the microscopic level, the difference is associated with the relative importance of *s* and *p* electrons in valence interactions.

Zr_2Al was selected for study for several reasons. First, Zr_2Al is a reasonably stable high-temperature material (*4*), being some-

* Current address: Department of Chemistry, SUNY-B, Binghamton, New York 13901.

† To whom correspondence should be addressed.

‡ Current address: Electronic and Information Technologies Laboratory, 3M Center, St. Paul, Minnesota 55144.

0022-4596/85 $3.00

TABLE I

Lattice constants	a = 489.4 pm
	c = 592.8 pm
Muffin-tin sphere radii:	Zr: 148.4 pm
	Al: 127.0 pm
Zr(1)–Al distances	318.7 pm (6×)
Zr(1)–Zr distances	296.4 pm (2×)
	318.7 pm (6×)
Zr(2)–Al distances	282.2 pm (3×)
	296.4 pm (2×)
Zr(2)–Zr distances	318.7 pm (6×)
Al–Zr distances	318.7 pm (6×)
	282.2 pm (3×)
	296.4 pm (2×)
% Filling of unit cell by muffin-tin spheres	58.58%

what typical of the zirconium aluminides. Second, the band structure of ZrS has been previously studied in two crystalline modifications (*5*), making possible a comparison of the roles of Zr in the sulfides and aluminides. Finally, Zr_2Al has a simple structure type, the Ni_2In-type, which is a structure type that is obtained from the NiAs-type by filling the trigonal-bipyramidal holes. Since the electronic structures of NiAs-type compounds have been extensively discussed and have been the subject of some recent band-structure calculations (*6*), it is of interest to calculate the electronic structure for a Ni_2In-type material for comparison purposes.

Calculations

The electronic structure was calculated by the Korringa–Kohn–Rostoker (KKR) method (*7*). The muffin-tin potential was obtained from the superposition of atomic charge densities calculated by the self-consistent Hartree–Fock–Slater method using a variation of the Herman and Skillman program (*8*). The procedure followed is that developed by Mattheiss (*9*). The crystal potential was taken to consist of a Coulombic component, the spherical part of the combination of atomic Coulombic potentials (*10*), and an exchange component calculated using Slater's free-electron exchange (*11*).

The wavefunctions and eigenvalues were determined by the Green's function method using the Ames Laboratory KKR programs based upon the discussion of Ham and Segall (*12*). The input information for the KKR calculations is summarized in Table I. The unit cell contains two formula units arranged as shown in Fig. 1.

Within each muffin-tin sphere the wavefunction corresponding to the eigenvalue E at the Brillouin zone (BZ) point k is expanded in spherical harmonics as

$$\Psi_{(\mathbf{k},E,\mathbf{r})}^{\text{muffin-tin}} = \sum_L C_L(\mathbf{k},E) f_l(E,r) Y_L(\mathbf{r})$$

where L is an index representing the angular momentum components (l,m), f_l is a solution to the radial Schrödinger equation, and C_L is an expansion coefficient. The expansion included spherical harmonics

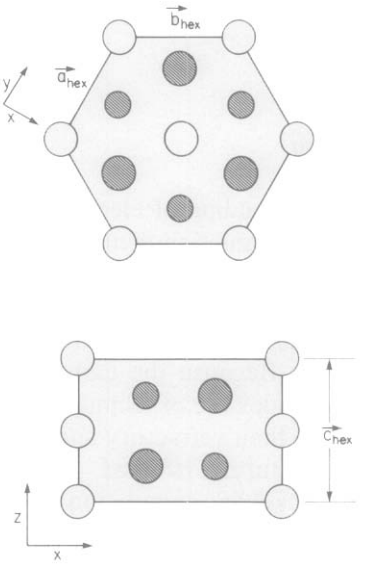

FIG. 1. The Zr_2Al (Ni_2In-type) structure. Top: view along the c axis, large circles indicate the Zr positions, small circles indicate the Al positions, shaded circles at $z = \frac{1}{2}$, open circles at $z = 0$. Bottom: view of the 110 plane, c axis vertical.

through $l = 2$ within the Zr spheres and through $l = 1$ in the Al sphere. The calculation was nonrelativistic and nonself-consistent. The wavefunctions and eigenvalues were calculated for 63 general k points and 6 high-symmetry points in the unique $\frac{1}{24}$ of the Brillouin zone. The calculations were carried out for 18 bands in the energy range between 0 and 1.2 Ry (1 Ry = 13.6 eV).

The electronic density of states (DOS) is given

$$N(\varepsilon) = \int_{BZ} d^3k\delta(\varepsilon(\mathbf{k}) - \varepsilon).$$

One way to calculate the DOS for a finite sample of points in the BZ is to use a histogram technique. In this procedure the number of eigenvalues between the energies of ε and $\varepsilon + \Delta\varepsilon$ are counted for all points in the BZ. In practice, since our sample is restricted to the unique or irreducible unit of the BZ (the IBZ), the DOS takes the form

$$N(\varepsilon) = \sum_{\substack{k\varepsilon IBZ \\ \varepsilon\le\varepsilon(\mathbf{k})\le\varepsilon+\Delta\varepsilon}} w(k)$$

where the weight, W, is determined by the number of points in the star of $\mathbf{k}$.

The angular decomposed DOS is calculated similarly. The angular decomposed DOS defined for a particular angular momentum l in a particular muffin–tin sphere by

$$N_l(\varepsilon) = \int_{BZ} d^3kQ_l(\varepsilon,k)\delta(\varepsilon(\mathbf{k}) - \varepsilon)$$

where

$$Q_l(\varepsilon,k) = \sum_m C^*_{l,m}(\varepsilon,k)C_{l,m}(\varepsilon,k) \int_0^{R_{ws}} r^2drf_l^2(\varepsilon,r).$$

In the histogram procedure, the integral is replaced by the sum

$$N_l(\varepsilon) = \sum_{\substack{k\varepsilon IBZ \\ \varepsilon\le\varepsilon(\mathbf{k})\le\varepsilon+\Delta\varepsilon}} Q_l(\varepsilon,k)W(k).$$

In the present calculation $\Delta\varepsilon$ was $2mRy$.

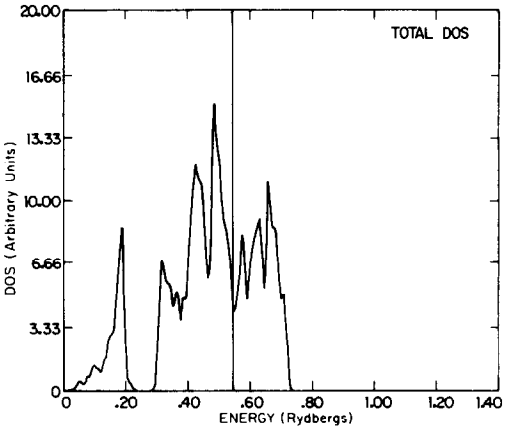

FIG. 2. The calculated DOS for Zr_2Al, the vertical line at 0.52 Ry indicates the Fermi energy.

The charge densities within each muffin–tin sphere within the energy intervals $0 \le \varepsilon \le 0.22$ Ry and $0.22 < \varepsilon \le E_F$ (see below) were obtained from the expression

$$\rho(\mathbf{r}) = \sum_L \rho_L(r)Y_L(\mathbf{r}).$$

The only nonvanishing elements of ρ_L for the expansion of the charge density occur for $(l,m) = (0,0)$, $(2,0)$, $(4,0)$, and $(4,3)$ at the Zr(1) site (D_{3d} symmetry), for $(0,0)$, $(2,0)$, $(4,0)$, and $(3,3)$ at the Zr(2) site (D_{3h} symmetry), and for $(0,0)$ and $(2,0)$ for the Al site (also D_{3h} symmetry). The nonvanishing elements were constructed in accordance with

$$\rho_L(r) = \sum_{E_{min}E<E_{max}} \sum_{L_1L_2} I^L_{L_1L_2}f_{l_1}(r)f_{l_2}(r)C^*_{L_1}(E)C_{L_2}(E)$$

where $I^L_{L_1L_2}$, the Gaunt coefficient, is given by

$$I^L_{L_1L_2} = \int Y^*_{L_1}Y_{L_2}Y^*_L d\Omega.$$

Results

The total DOS Zr_2Al is shown in Fig. 2. The states below the Fermi energy are considered in two ranges: the range between 0

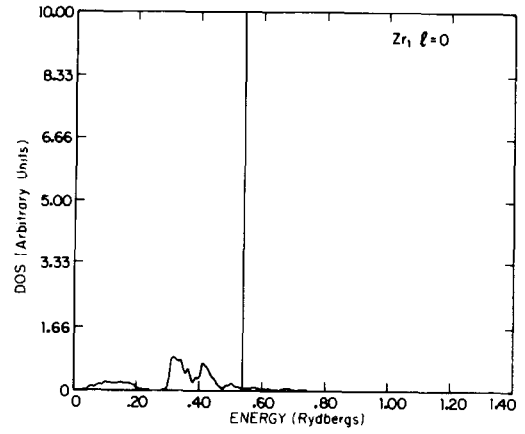

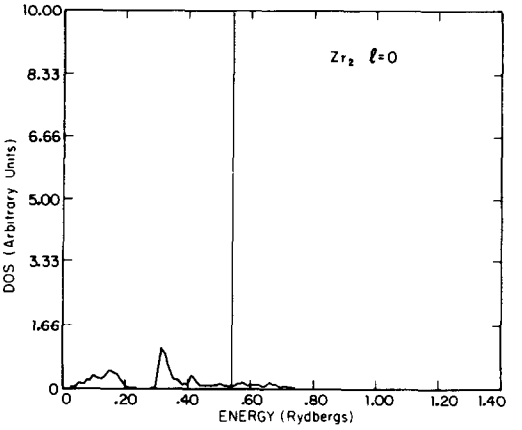

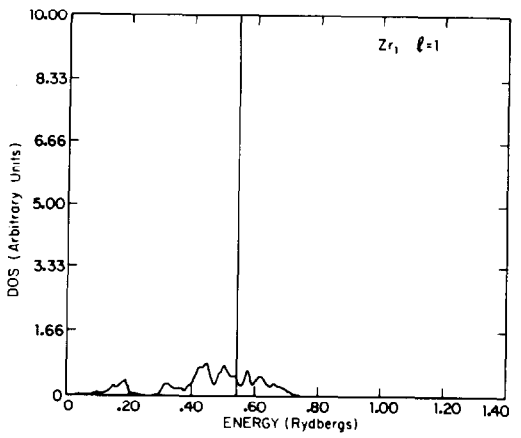

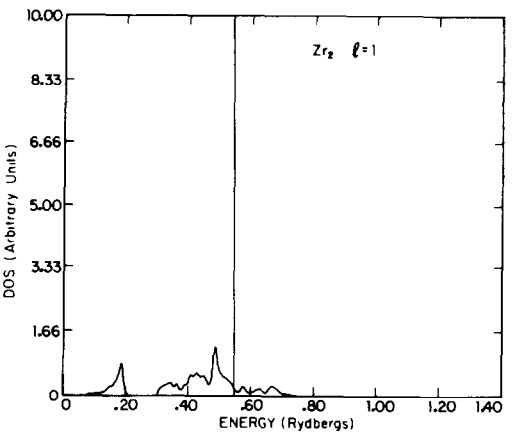

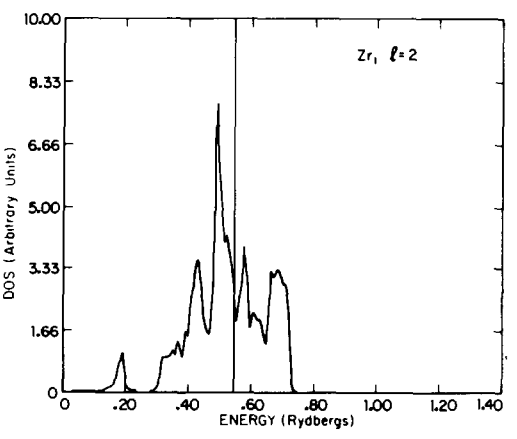

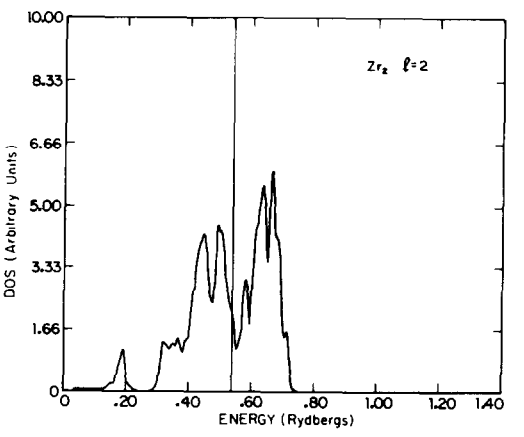

FIG. 3. The *l*-decomposed DOS for Zr(1) (large open circles of Fig. 1).

FIG. 4. The *l*-decomposed DOS for Zr(2) (large shaded circles of Fig. 1).

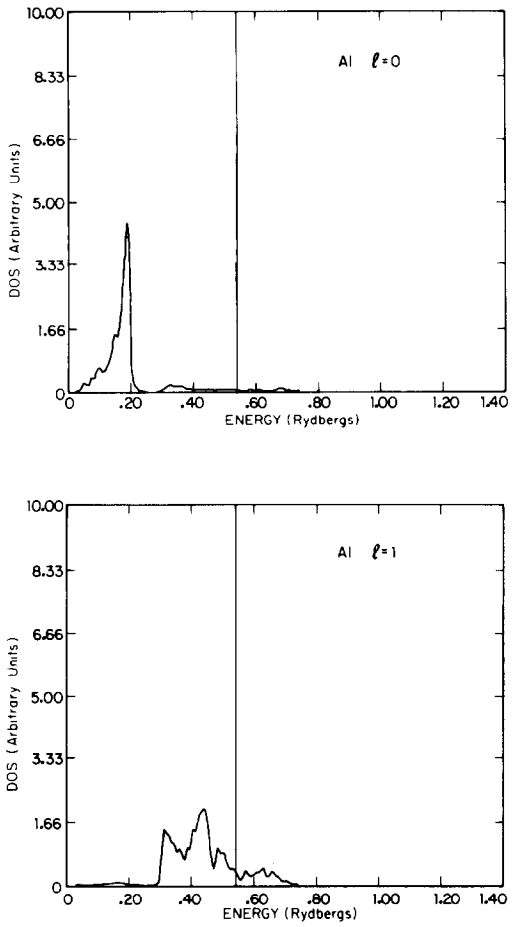

FIG. 5. The l-decomposed DOS for Al (small shaded circles of Fig. 1).

and 0.22 Ry and at higher energies but below E_F. Those states in the 0 to 0.22 Ry interval will be called valence band (VB) states, and the occupied states at higher energies will be called conduction band (CB) states.

The total DOS is decomposed into partial, angular-momentum labeled DOS curves which are shown for Zr(1) (Fig. 3), Zr(2) (Fig. 4), and Al (Fig. 5). The Zr (l = 0, 1, and 2)-type states are distributed over both VB and CB regions with the principal contribution to the states in the CB region being made by the Zr (l = 2)-type states. The Al (l = 0)-type states are concentrated in the VB region and the Al (l = 1)-type states are concentrated in the CB region.

Electron densities ($\Psi^*\Psi$) were calculated as functions of position and evaluated at the surfaces of the muffin–tin spheres. These electron densities have been graphed in selected planes using polar coordinates. Figure 6 shows the trace of the VB muffin–tin sphere-surface density in the xy plane for Zr(2). The directions for the orthogonal coordinates, x, y, and z, are those of the orthorhombic cell (the so-called orthohexagonal cell) as shown in Fig. 1, and the origin is the same as that for the hexagonal cell. The information concerning the muffin–tin sphere and the plane of intersection for Figs. 7–10 is given in Table II. The asphericities of the electron densities are taken as evidence of the directional interactions. Taken in total Figs. 6–10 show that the VB states centered upon Zr generally

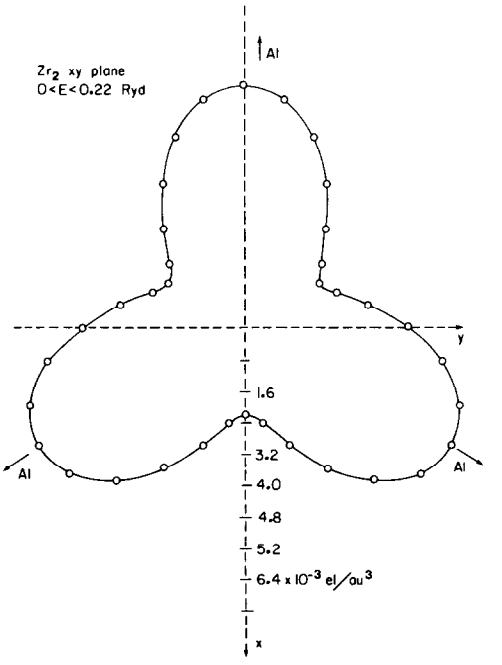

FIG. 6. The calculated electron density on the intersection of the Zr(2) muffin–tin sphere with the $z = \frac{1}{4}$ plane, VB states only.

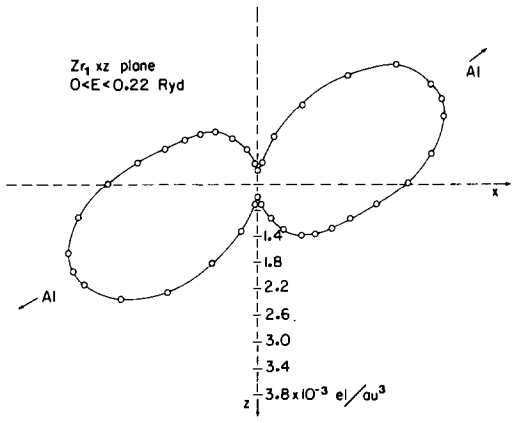

FIG. 7. The calculated electron density on the intersection of the Zr(1) muffin-tin sphere with the $y = 0$ plane, VB states only.

contribute to direct Zr–Al interactions (show pronounced maxima along the Zr to Al vectors) and do not contribute to direct Zr–Zr interactions (show minima along the Zr to Zr vectors). On the other hand, the

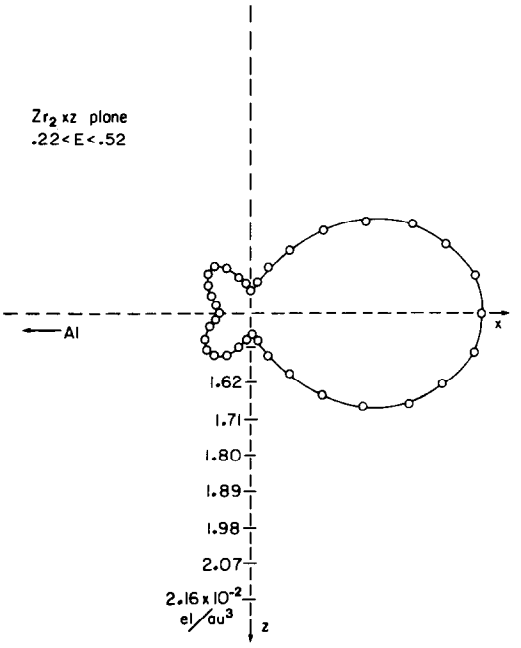

FIG. 8. The calculated electron density on the intersection of the Zr(2) muffin-tin sphere with the $y = 0$ plane, CB states only.

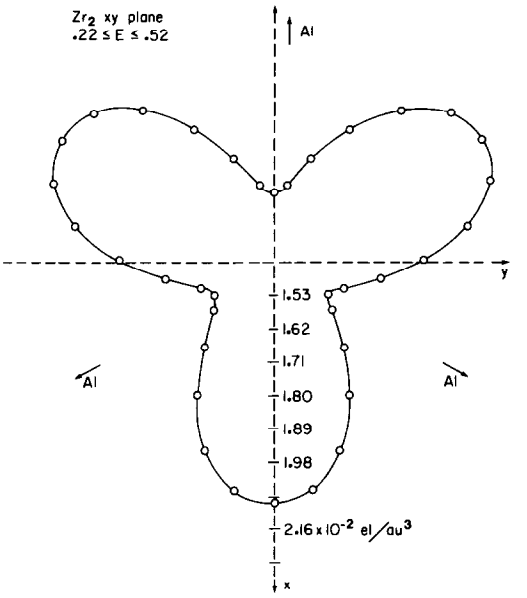

FIG. 9. The calculated electron density on the intersection of the Zr(2) muffin-tin sphere with the $z = \frac{1}{4}$ plane, CB states only.

opposite is true for the CB states, namely the Zr-centered states in the CB region (principally *d* type) contribute significantly to Zr–Zr interactions and negligibly to Zr–Al interactions.

Special attention is called to the fact that the contribution of states centered upon Al to the VB is principally from Al *s*-type states (Fig. 5) and thus that the contribution of Al-centered states to the VB is nondirectional. In fact, the overall contribution of Al centered states is not significantly direc-

TABLE II

ELECTRON DENSITIES AT THE INTERSECTION OF THE MUFFIN-TIN SPHERES WITH PLANES FOR STATES IN THE CB AND VB REGIONS

Energy region	Plane	Atom	Figure
VB	*xy*	Zr(2)	6
VB	*xz*	Zr(1)	7
CB	*xz*	Zr(2)	8
CB	*xy*	Zr(2)	9
CB	*xz*	Zr(1)	10

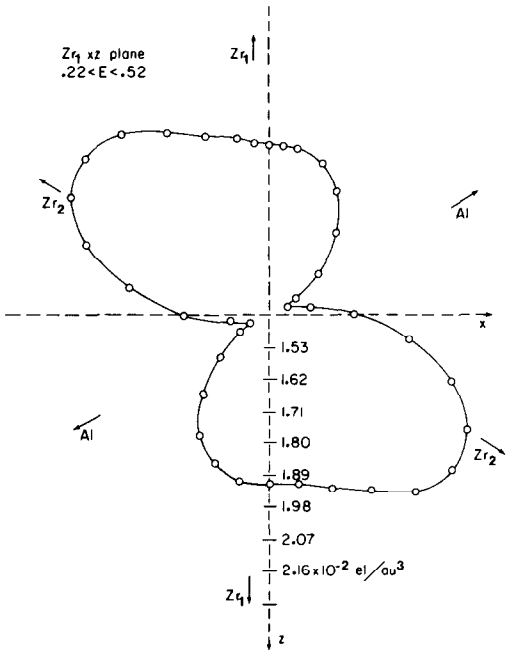

FIG. 10. The calculated electron density on the intersection of the Zr(1) muffin–tin sphere with the $y = 0$ plane, CB states only.

tional character, for the total electron densities at the Al muffin–tin sphere boundary were found to deviate negligibly from spherical symmetry.

Conclusions

The bonding in Zr_2Al is thus seen to consist of two principal parts, a VB part peaking at about 0.34 Ry (4.6 eV) below E_F which has a major contribution from the Al *s*-type orbitals, and a CB part which falls between E_F and $E_F - 0.24$ Ry (3.3 eV) and consists primarily of Zr *d*-type orbitals. The interaction between the *s*-type orbitals on the main-group element and transition-metal-centered orbitals in the VB region is a result that is significantly different from that previously obtained for sulfides, as is discussed further below.

The calculation of numbers of electrons within the Wigner–Seitz spheres permits the breakdown given in Table III. The Wigner–Seitz spheres are defined so that the total volume of the spheres within a unit cell is equal to the volume of the unit cell. Since the Al *p*-type contribution falls almost entirely within the CB region, and since in this region the electron densities centered on Zr(1) and Zr(2) are directed so as to evade the Al positions, it is concluded that the Al-centered *p*-type states are principally non- or antibonding in Zr_2Al.

Furthermore, the Al–Al distances in Zr_2Al are all greater than 409.5 pm (7.74 au), a distance that precludes substantial Al–Al interaction. For example, the Pauling bond order for the shortest Al–Al distance is 0.002. These facts, together with the large Zr *d*-type DOS at E_F demonstrates that the metallic character of Zr_2Al derives principally from Zr *d*-type states. The results reported here may be compared with those previously obtained for ZrS in the WC- and NaCl-type structures (*5*). In the sulfide cases the VB (defined similarly to that defined here) states are principally sulfur *p*-type and the CB states are principally Zr *d*-type. The major differences, then, between Zr_2Al and ZrS lie in the nature of the "nonmetal" contributions to the VB (*s*-type in Zr_2Al and *p*-type in ZrS) and in the contribution of non- or antibonding states to the CB. In the case of Zr_2Al the Al *p*-type electrons are principally nonbonding, since 83.5% of the ca. 1.3 *p*-type states centered on Al fall in the CB region.

Comparison with the results of the calculation for TiS and VS in the NiAs-type structure is of interest. In these NiAs-type

TABLE III

STATE TYPE IN THE VB AND CB REGIONS AS PERCENTAGES

	Al-*s*	Al-*p*	Zr-*s*	Zr-*p*	Zr-*d*
VB	45.4	11.6	15.4	12.4	15.2
CB	0.80	12.2	9.1	11.5	66.4

solids, as in ZrS, the sulfur *s*-type states fall about 1 Ry (13.6 eV) below E_F in a region to which the transition-metal atoms make very small contributions, and the VB region at about 0.4 Ry (5.4 eV) below E_F is made up principally of sulfur *p*-type states. Thus, a major influence upon the difference between the sulfides and aluminides of the early transition metal is seen to be, as expected, the difference in the electronegativities of the main-group elements which has the effect of raising the Al *s*- and *p*-type orbitals relative to those of sulfur, thereby resulting in differing valence interactions.

Acknowledgments

The Ames Laboratory is operated for the U.S. Department of Energy by Iowa State University under Contract W-7405-Eng-82. This research was supported by the Office of Basic Energy Sciences, Materials and Sciences Division.

References

1. A. Neckel, P. Rastl, R. Eibler, P. Weinberger, and K. Schwarz, *J. Phys. C. Solid State Phys.* **9,** 579 (1976).
2. M. Gupta, V. A. Gubanova, and D. E. Ellis, *J. Phys. Chem. Solids* **8,** 499 (1977).
3. V. L. Moruzzi, A. R. Williams, and J. F. Janak, *Phys. Rev. B.* **10,** 4856 (1974).
4. R. J. Kematick and H. F. Franzen, *J. Solid State Chem.* **54,** 226 (1984).
5. T.-H. Nguyen, H. Franzen, and B. N. Harmon, *J. Chem. Phys.* **73,** 425 (1980).
6. J. Nakahara, H. Franzen, and D. Misemer, *J. Chem. Phys.* **76,** 4080 (1982).
7. W. Kohn and N. Rostoker, *Phys. Rev.* **94,** 1111 (1954).
8. F. Herman and S. Skillman, "Atomic Structure Calculations," Prentice-Hall, Englewood Cliffs, N.J. (1963).
9. L. F. Mattheiss, *Phys. Rev.* **133,** 184 (1963).
10. P. O. Lowdin, *Adv. Phys.* **6,** 1 (1956).
11. J. C. Slater, *Phys. Rev.* **81,** 385 (1951).
12. F. S. Ham and B. Segall, *Phys. Rev.* **124,** 1786 (1961).